

Box²EL: Concept and Role Box Embeddings for the Description Logic \mathcal{EL}^{++}

Mathias Jackermeier¹, Jiaoyan Chen² and Ian Horrocks¹

¹Department of Computer Science, University of Oxford

²Department of Computer Science, The University of Manchester

Abstract

Representation learning in the form of semantic embeddings has been successfully applied to a variety of tasks in natural language processing and knowledge graphs. Recently, there has been growing interest in developing similar methods for learning embeddings of entire ontologies. We propose Box²EL, a novel method for representation learning of ontologies in the Description Logic \mathcal{EL}^{++} , which represents both concepts and roles as boxes (i.e. axis-aligned hyperrectangles), such that the logical structure of the ontology is preserved. We theoretically prove the soundness of our model and conduct an extensive empirical evaluation, in which we achieve state-of-the-art results in subsumption prediction, link prediction, and deductive reasoning. As part of our evaluation, we introduce a novel benchmark for evaluating \mathcal{EL}^{++} embedding models on predicting subsumptions involving both atomic and complex concepts.

1 Introduction

Recent years have seen tremendous interest in semantic embeddings, i.e. representing symbolic data in a vector space such that their semantics and relationships are preserved. These methods achieved their first great successes in natural language processing, where learned embeddings of words and phrases in text corpora have proven to be effective at a wide variety of tasks [Mikolov *et al.*, 2013]. Semantic embeddings have also been applied to Knowledge Graphs (KG), i.e. multi-relational graph-structured data, often organized as RDF triples,¹ such as DBpedia [Lehmann *et al.*, 2015] and Wikidata [Vrandečić and Krötzsch, 2014]. In this context, KG embedding (KGE) methods such as TransE [Bordes *et al.*, 2013], TransH [Wang *et al.*, 2014], and DistMult [Yang *et al.*, 2015] are widely employed for common tasks in KG construction and curation, such as link prediction and entity resolution [Wang *et al.*, 2017; Hogan *et al.*, 2021].

Ontologies² are also widely used for representing knowledge, but usually for conceptual knowledge of a domain such

as (hierarchical) clinical terms and food categorizations. The Web Ontology Language (OWL) is widely adopted in domains such as the Semantic Web and Bioinformatics [Baader *et al.*, 2005b; Staab and Studer, 2010]; it is underpinned by a Description Logic (DL) with formal semantics. Semantic embeddings have been applied to ontologies, but investigations are still relatively preliminary, especially for OWL ontologies. Some embedding solutions, including box lattice embeddings [Vilnis *et al.*, 2018] and hyperbolic embeddings [Nickel and Kiela, 2017], can only consider an ontology’s concept hierarchy, while some OWL ontology embedding methods, such as OPA2Vec [Smaili *et al.*, 2019] and OWL2Vec* [Chen *et al.*, 2021], pay little attention to the logic and instead rely on literals such as labels and comments.

Some methods have been proposed for embedding the DL semantics of OWL ontologies, mostly aiming at the \mathcal{EL}^{++} fragment of OWL. Since \mathcal{EL}^{++} represents complex logical relationships, more complex geometric models are required. ELEm [Kulmanov *et al.*, 2019] and its variant EmEL⁺⁺ [Mondal *et al.*, 2021] use high-dimensional balls instead of points to represent \mathcal{EL}^{++} concepts, leading to better axiom prediction and deductive inference performance than KGEs. However, a drawback of this ball representation is that it is not closed under concept intersection, which led to the development of BoxEL [Xiong *et al.*, 2022] and ELBE [Peng *et al.*, 2022], which use axis-aligned hyperrectangles (i.e., boxes) as concept representations. Although these methods effectively represent the concepts, they still use a single translation vector to model the relation like TransE. This limits expressivity and can represent only one-to-one relations.

In this work we propose to represent both concepts and relations by boxes, and develop a more robust \mathcal{EL}^{++} embedding method named Box²EL. Motivated by BoxE [Abboud *et al.*, 2020], Box²EL represents each binary relation (role) by a head box and a tail box, and adopts so-called bump vectors to translate the box embedding of a concept w.r.t. other concepts that co-occur in an axiom. We have developed an effective training method for our model, and have theoretically proven the soundness of Box²EL, i.e., the learned embeddings can completely capture the semantics of an \mathcal{EL}^{++} ontology. We have also conducted a more comprehensive evaluation than previous works. Three real-life ontologies are

¹Resource Description Framework. <https://www.w3.org/RDF/>

²Ontologies are sometimes regarded as a kind of KG; for clarity, we use KG to refer to only graphs mainly composed of relational facts

with optional (and simple) schemas or constraints.

used to fully explore the potential of Box²EL and several other \mathcal{EL}^{++} embedding methods on predicting subsumption and role assertion axioms, and on approximating deductive reasoning. Moreover, while previous works only predicted subsumptions between named concepts, we consider subsumptions of multiple forms involving complex concepts and logical operations. Assertion axiom prediction (a.k.a. link prediction) is conducted on the Gene Ontology (GO) and the STRING database for the real-world application of protein-protein interaction (PPI) prediction. In all of our experiments, Box²EL generally achieves better performance than the previous methods.

2 Preliminaries

2.1 Description Logic \mathcal{EL}^{++}

The DL \mathcal{EL}^{++} [Baader *et al.*, 2005a] underpins the OWL 2 EL profile recommended by W3C.³ It has been widely adopted by many real-life large-scale ontologies due to its relative high expressivity and tractability (polynomial time for standard reasoning tasks). Given a signature composed of atomic (or named) concepts \mathcal{N}_C , atomic roles \mathcal{N}_R , and individuals \mathcal{N}_I , an \mathcal{EL}^{++} concept is recursively defined as

$$\top \mid \perp \mid A \mid C \sqcap D \mid \exists r.C \mid \{a\}$$

where \top is the top concept, \perp is the bottom concept, $A \in \mathcal{N}_C$ is an atomic concept, $r \in \mathcal{N}_R$ is an atomic role, $a \in \mathcal{N}_I$ is an individual, and C and D are themselves \mathcal{EL}^{++} concepts. An \mathcal{EL}^{++} ontology \mathcal{O} consists of a TBox \mathcal{T} and an ABox \mathcal{A} . Briefly, a TBox is a set of General Concept Inclusion axioms (subsumptions) of the form $C \sqsubseteq D$, where C and D are \mathcal{EL}^{++} concepts; an ABox is a set of concept and role assertion axioms of the form $C(a)$ and $r(a, b)$, respectively, where C is an \mathcal{EL}^{++} concept, r is an \mathcal{EL}^{++} role and a, b are \mathcal{EL}^{++} individuals.⁴

Example 1. *The following ontology models a simple family domain:*

$$\begin{aligned} \mathcal{T} &= \{\text{Father} \sqsubseteq \text{Parent} \sqcap \text{Male}, \text{Child} \sqsubseteq \exists \text{hasParent.Father}\} \\ \mathcal{A} &= \{\text{Father}(\text{Alex}), \text{Child}(\text{Bob}), \text{hasParent}(\text{Bob}, \text{Alex})\} \end{aligned}$$

The TBox specifies that a father is a male parent and every child has a father, while the ABox contains concrete data.

Semantics. Similarly to first order logic, the semantics of \mathcal{EL}^{++} are defined in terms of *interpretations* that map individuals to elements, concept names to subsets, and role names to binary relations over some set called the *interpretation domain*. An interpretation \mathcal{I} that satisfies the semantics of every axiom in \mathcal{O} is called a *model* of \mathcal{O} , denoted as $\mathcal{I} \models \mathcal{O}$. For a formal definition and more details, please refer to [Baader *et al.*, 2005a].

2.2 Knowledge Graph Embeddings

A KGE represents entities and relations by vectors with their relationships preserved in the vector space. For example, considering the embeddings of a KG by TransE [Bordes *et al.*,

2013], we have $v(h) + v(r) \approx v(t)$ for each triple (h, r, t) , where $v(\cdot)$ denotes the embedding, i.e., vector representation. One widely adopted embedding paradigm is to define a score function for modeling the plausibility of a triple, and iteratively adjust the embeddings to minimize some loss on both positive and negative triples via an optimization algorithm. According to how the triple is modeled, we can divide these methods into *translational models*, which use geometric distances (e.g., TransE), *bilinear models*, which use matrix multiplications (e.g., DistMult [Yang *et al.*, 2015]), and *neural models*, which use neural networks (e.g., ConvE [Dettmers *et al.*, 2018]). Another paradigm is pipeline-based and first transforms facts into sequences before applying a word embedding model; a typical example is RDF2Vec, which uses random walks and Word2Vec [Ristoski and Paulheim, 2016].

The pipeline-based paradigm cannot strictly keep the relationships of the KG, but only captures co-occurrence and correlation, while bilinear models and neural models are less interpretable and often more complicated than translational models. Thus translational models become the most suitable for embedding DLs and in fact are adopted by the majority of the current methods. However, modeling a relation by one simple translation vector as in TransE cannot deal with one-to-many, many-to-one, and many-to-many relations. To address this problem, several TransE extensions such as TransH [Wang *et al.*, 2014] and TransR [Lin *et al.*, 2015] project the entity embeddings to some relation-specific space before computing translations. Another approach is employed by the recent method BoxE [Abboud *et al.*, 2020; Messner *et al.*, 2022], which adopts n boxes to represent each n -ary relation and uses the idea of bump vectors to model the association between head and tail entities. In this work we extend and apply the relation representation idea of BoxE together with box-based concept representations for embedding ontologies of the DL \mathcal{EL}^{++} , which have more complex logical structure than KGs.

2.3 Description Logic Embeddings

Most DL embedding methods target the DL \mathcal{EL}^{++} . The early method ELEM [Kulmanov *et al.*, 2019] represents concepts as high-dimensional balls with a vector for the center and a real value for the radius, and roles as translational vectors. Points inside a ball are regarded as instances of the corresponding concept; concept subsumption in the form of $C \sqsubseteq D$ is modeled as ball inclusion, and subsumptions involving existential restriction $\exists r.C$ are modeled by translating the ball center along the vector of r . The embeddings are learned by minimizing a loss on positive TBox axioms and randomly sampled negative axioms in the form of $C \not\sqsubseteq \exists r.D$. Note that the intersection of two balls is in general not a ball itself, and axioms of the form $C \sqcap D \sqsubseteq E$ are modeled by only an approximation of proper ball inclusion. EmEL⁺⁺ [Mondal *et al.*, 2021] extends ELEM with \mathcal{EL}^{++} role inclusion and role chain constructs.

To ensure the closure of concept representations under intersection, BoxEL [Xiong *et al.*, 2022] and ELBE [Peng *et al.*, 2022] extend ELEM by representing concepts as axis-parallel boxes with two vectors for either the lower and upper corners or the center and offset. However, their role repre-

³https://www.w3.org/TR/owl2-profiles/#OWL_2_EL

⁴ \mathcal{EL}^{++} supports a few additional axioms that we do not detail here as they are currently not considered by Box²EL.

sensation also follows TransE: each role is represented with a single vector and subsumptions involving $\exists r.C$ are modeled by translating the box corners (or center). This approach cannot support one-to-many, many-to-one and many-to-many relations [Wang *et al.*, 2014; Lin *et al.*, 2015]. As theoretically analyzed in [Gutiérrez-Basulto and Schockaert, 2018], convex regions are instead required to fully capture the semantics of DLs, and single vectors do not have sufficient representation capability. Going beyond \mathcal{EL}^{++} , Embed2Reason [Garg *et al.*, 2019] is a method that learns embeddings for the DL \mathcal{ALC} based on quantum logic, but its focus lies on ABox reasoning and traditional KG completion.

Meanwhile, the evaluation of current \mathcal{EL}^{++} embedding works is often incomplete. Except for [Mondal *et al.*, 2021], they all ignore deductive reasoning, and only test simple subsumptions between named concepts in the prediction setting, while more complicated axioms such as subsumptions involving existential restrictions have not yet been investigated.

3 Method

In this section, we describe the geometric representation employed by Box²EL and the training procedure for learning embeddings of a given ontology. We also show that our model is *sound* in that it corresponds to logical models of \mathcal{EL}^{++} .

3.1 Geometric Representation

Given an ontology \mathcal{O} with signature $\Sigma = (\mathcal{N}_C, \mathcal{N}_R, \mathcal{N}_I)$, we need to specify how concepts, roles, and individuals are mapped to the geometric embedding space \mathbb{R}^n . First, we make use of nominals (i.e., concepts of the form $\{a\}$ for an individual a) to treat individuals like concepts and convert ABox axioms into semantically equivalent TBox axioms with the following transformations:

$$\begin{aligned} C(a) &\rightsquigarrow \{a\} \sqsubseteq C \\ r(a, b) &\rightsquigarrow \{a\} \sqsubseteq \exists r.\{b\} \end{aligned}$$

Concept Representation

We follow recent work [Xiong *et al.*, 2022; Peng *et al.*, 2022] and represent concepts as n -dimensional *boxes*, i.e. *axis-aligned hyperrectangles*. This representation has several advantages over the alternative based on n -dimensional *balls*, such as closure under concept intersection, and has been shown to work well in practice [Peng *et al.*, 2022].

Formally, let $\mathcal{N}'_{CI} \subseteq \mathcal{N}_C \cup \bigcup_{a \in \mathcal{N}_I} \{\{a\}\}$ be the set of named concepts and nominals of named individuals that occur in \mathcal{O} . We associate with every concept $C \in \mathcal{N}'_{CI}$ two vectors $\mathbf{l}_C \in \mathbb{R}^n$ and $\mathbf{u}_C \in \mathbb{R}^n$ such that $\mathbf{l}_C \leq \mathbf{u}_C$, where \leq is applied element-wise. These vectors form the *lower* and *upper* corner of the box of C , i.e., $\text{Box}(C) = \{x \in \mathbb{R}^n \mid \mathbf{l}_C \leq x \leq \mathbf{u}_C\}$. The *center* of $\text{Box}(C)$ is given by $(\mathbf{l}_C + \mathbf{u}_C)/2$, and its *offset* is $(\mathbf{u}_C - \mathbf{l}_C)/2$.

Role Representation

While most existing \mathcal{EL}^{++} embedding models represent roles (binary relations) via simple translations in the form of TransE [Bordes *et al.*, 2013], we instead follow the idea of the BoxE KGE model [Abboud *et al.*, 2020]. That is, we associate every role $r \in \mathcal{N}'_R$ in the set of roles $\mathcal{N}'_R \subseteq \mathcal{N}_R$ occurring in \mathcal{O} with a *head box* $\text{Head}(r)$ and a *tail box* $\text{Tail}(r)$.

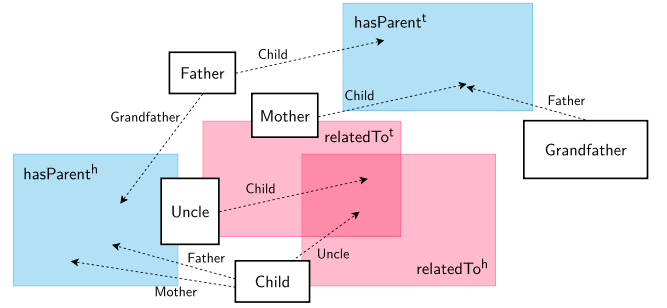


Figure 1: An illustration of Box²EL. White boxes represent concept embeddings, whereas role embeddings are illustrated as shaded boxes and labelled as r^h or r^t for the head or tail box of r , respectively. Bump vectors are drawn as arrows and labelled with the corresponding concept.

Intuitively, every point in the head box is related via r to every point in the tail box. To make this representation more expressive, we introduce bump vectors $\text{Bump}(C)$ for every concept C , which model the interactions between concepts and dynamically move the position of the embeddings of related concepts. An axiom of the form $C \sqsubseteq \exists r.D$ is then considered to hold if

$$\text{Box}(C) + \text{Bump}(D) \subseteq \text{Head}(r)$$

and

$$\text{Box}(D) + \text{Bump}(C) \subseteq \text{Tail}(r),$$

where $A + t$ denotes the translation of box A along vector t .

Example 2. Consider the following TBox \mathcal{T} :

$\text{Child} \sqsubseteq \exists \text{hasParent.Mother}, \quad \text{Child} \sqsubseteq \exists \text{hasParent.Father},$
 $\text{Child} \sqsubseteq \exists \text{relatedTo.Uncle}, \quad \text{Uncle} \sqsubseteq \exists \text{relatedTo.Child},$
 $\text{Father} \sqsubseteq \exists \text{hasParent.Grandfather}, \quad \text{Mother} \sqcap \text{Father} \sqsubseteq \perp$

Figure 1 illustrates a 2-dimensional Box²EL model that correctly represents the axioms in \mathcal{T} .

Expressiveness. As demonstrated by the previous example, the expressive role representation employed by Box²EL allows modeling *one-to-many* relations such as *hasParent* and symmetric relations like *relatedTo*, overcoming the fundamental limitations of TransE. This is similar to the setting of KGEs, in which the underlying BoxE representation can be shown to be *fully expressive*, i.e., able to correctly model any arbitrary set of facts [Abboud *et al.*, 2020].

Model complexity. Box²EL requires $2n|\mathcal{N}'_{CI}|$ parameters to store the lower and upper corners of the box embeddings of concepts and individuals. In order to represent the head and tail boxes for every relation and a bump vector per concept, the model needs $4n|\mathcal{N}'_R| + n|\mathcal{N}'_{CI}|$ additional parameters. Therefore, the total space complexity of Box²EL is in $O(n(3|\mathcal{N}'_{CI}| + 4|\mathcal{N}'_R|))$.

3.2 Training Procedure

In order to learn embeddings for a given \mathcal{EL}^{++} ontology \mathcal{O} , we follow the framework introduced by [Kulmanov *et al.*, 2019]. That is, we transform \mathcal{O} into a set of axioms in normal

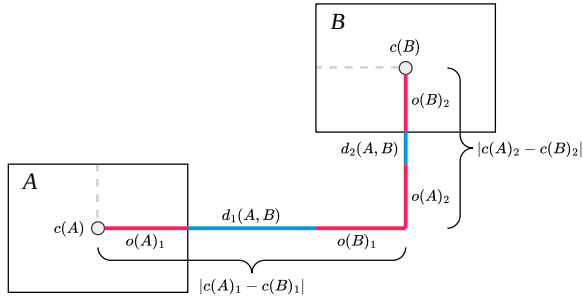


Figure 2: Calculating the element-wise distance $d(A, B)$ between two boxes A and B from their centers and offsets.

form using the normalization procedure described in [Baader *et al.*, 2005a] and introduce a separate loss function for each normal form. During training, we optimize the corresponding loss function for every axiom in \mathcal{O} .

Loss Functions

Our loss functions follow the distance-based loss formulation in [Kulmanov *et al.*, 2019; Peng *et al.*, 2022] and aim to minimize the element-wise distance between the embeddings of related concepts. Given two arbitrary boxes A and B , this element-wise distance is computed as

$$d(A, B) = |c(A) - c(B)| - o(A) - o(B),$$

where $c(\cdot)$ and $o(\cdot)$ denote the center and offset of a box, respectively. See Figure 2 for an illustration.

Generic inclusion loss. Before defining loss functions for the different \mathcal{EL}^{++} normal forms, we first introduce a generic inclusion loss $\mathcal{L}_{\subseteq}(A, B)$. It encourages box A to be contained in box B and is defined as

$$\mathcal{L}_{\subseteq}(A, B) = \|\max\{\mathbf{0}, d(A, B) + 2o(A) - \gamma\}\|,$$

where γ is a margin hyperparameter. From Figure 2 we see that $\mathcal{L}_{\subseteq}(A, B) = 0$ if A lies within γ -distance of B in each dimension.

We next introduce each normal form and the corresponding loss function. Note that all concepts in the normal forms below are *atomic* concepts.

First normal form (NF1). For an NF1 axiom of the form $C \sqsubseteq D$, the learned embeddings need to satisfy $\text{Box}(C) \subseteq \text{Box}(D)$, corresponding to the semantics of concept inclusion. Therefore, we define the loss for NF1 as simply the inclusion loss:

$$\mathcal{L}_1(C, D) = \mathcal{L}_{\subseteq}(\text{Box}(C), \text{Box}(D)).$$

Second normal form (NF2). For an NF2 axiom of the form $C \sqcap D \sqsubseteq E$, we similarly require that the intersection of the boxes of C and D is a subset of the box of E . The intersection of $\text{Box}(C)$ and $\text{Box}(D)$ is itself a box with lower corner $\max\{\mathbf{l}_C, \mathbf{l}_D\}$ and upper corner $\min\{\mathbf{u}_C, \mathbf{u}_D\}$, where \max and \min are applied element-wise. We thus have

$$\mathcal{L}_2(C, D, E) = \mathcal{L}_{\subseteq}(\text{Box}(C) \cap \text{Box}(D), \text{Box}(E)).$$

However, this formulation is problematic since it can be easily minimized to 0 by setting $\text{Box}(C)$ and $\text{Box}(D)$ to be

disjoint. While disjoint embeddings for C and D would technically not violate the semantics, usually an axiom of the form $C \sqcap D \sqsubseteq \perp$ would have been used directly if it had been the intention that C and D should be disjoint. Therefore, we add the additional term

$$\|\max\{\mathbf{0}, \max\{\mathbf{l}_C, \mathbf{l}_D\} - \min\{\mathbf{u}_C, \mathbf{u}_D\}\}\|$$

to the loss, which intuitively encourages $\text{Box}(C) \cap \text{Box}(D)$ to be non-empty by making all elements of its offset vector positive.

Third normal form (NF3). For an NF3 axiom of the form $C \sqsubseteq \exists r.D$, the embeddings should satisfy $\text{Box}(C) + \text{Bump}(D) \subseteq \text{Head}(r)$ and $\text{Box}(D) + \text{Bump}(C) \subseteq \text{Tail}(r)$. This is captured by the following loss function:

$$\begin{aligned} \mathcal{L}_3(C, r, D) = & \frac{1}{2} \left(\mathcal{L}_{\subseteq}(\text{Box}(C) + \text{Bump}(D), \text{Head}(r)) \right. \\ & \left. + \mathcal{L}_{\subseteq}(\text{Box}(D) + \text{Bump}(C), \text{Tail}(r)) \right). \end{aligned}$$

Fourth normal form (NF4). For an NF4 axiom of the form $\exists r.C \sqsubseteq D$, we need to ensure that all points in the embedding space that are connected to C via role r are contained in $\text{Box}(D)$. It can be easily seen from our geometric representation that the set of these points is contained in the set $\text{Head}(r) - \text{Bump}(C)$. We therefore define the loss for the fourth normal form as

$$\mathcal{L}_4(r, C, D) = \mathcal{L}_{\subseteq}(\text{Head}(r) - \text{Bump}(C), \text{Box}(D)).$$

Fifth normal form (NF5). Axioms of the fifth normal form $C \sqcap D \sqsubseteq \perp$ state that concepts C and D are disjoint. Our corresponding loss function penalizes embeddings for which the element-wise distance is not greater than 0 (within a margin of γ) and is defined as

$$\mathcal{L}_5(C, D) = \|\max\{\mathbf{0}, -(d(\text{Box}(C), \text{Box}(D)) + \gamma)\}\|.$$

Sixth normal form (NF6). An NF6 axiom is of the form $\exists r.C \sqsubseteq \perp$ and thus requires $\exists r.C$ to be unsatisfiable. As with most previous approaches [Kulmanov *et al.*, 2019; Peng *et al.*, 2022], one limitation of our method is that we cannot easily model this requirement in the embedding space, since the learned embeddings of r and C are independent. As an approximation, we instead model the axiom $\exists r.\top \sqsubseteq \perp$ by defining the NF6 loss as

$$\mathcal{L}_6(r, C) = \|o(\text{Head}(r))\|.$$

This guarantees that $\exists r.C$ is unsatisfiable, but also makes every other concept $\exists r.X$ with $X \neq C$ unsatisfiable.

Seventh normal form (NF7). Finally, we adopt the following loss for an NF7 axiom of the form $C \sqsubseteq \perp$, which encourages $\text{Box}(C)$ to be empty:

$$\mathcal{L}_7(C) = \|o(\text{Box}(C))\|.$$

Negative Sampling

While the embeddings could in theory be directly optimized with the above loss functions, we additionally employ negative sampling to further improve the quality of the learned embeddings. We follow previous work [Kulmanov *et al.*, 2019;

Xiong *et al.*, 2022; Peng *et al.*, 2022] and generate negative samples for axioms of the form $C \sqsubseteq \exists r.D$ by replacing either C or D with a randomly selected different concept.

Our loss function for negative training examples is based on the *minimal distance* between any two points in two boxes A and B , defined as

$$\mu(A, B) = \|\max\{\mathbf{0}, d(A, B) + \gamma\}\|,$$

where γ is again a margin hyperparameter. Concretely, we introduce another hyperparameter, the *negative sampling distance* $\delta > 0$, and define the loss for a negative training example $C \not\sqsubseteq \exists r.D$ as

$$\begin{aligned} \mathcal{L}_{\not\sqsubseteq}(C, r, D) = & (\delta - \mu(\text{Box}(C) + \text{Bump}(D), \text{Head}(r)))^2 \\ & + (\delta - \mu(\text{Box}(D) + \text{Bump}(C), \text{Tail}(r)))^2. \end{aligned}$$

This formulation encourages the minimal distance between the bumped embedding of C and the head box of r , as well as the minimal distance between the bumped embedding of D and the tail box of r , to be close to the negative sampling distance δ . As desired, it thus makes the negative training example less likely to be induced by the model.

For every NF3 axiom we generate a new set of $\omega \geq 1$ negative samples in every epoch, where the number of negative samples ω is another hyperparameter. These negative training examples are then used in conjunction with the positive axioms to learn the embeddings.

Regularization

Finally, we combat overfitting of our expressive role representation by adding the regularization term

$$\lambda \sum_{C \in \mathcal{N}'_{CI}} \|\text{Bump}(C)\|$$

to the loss, where λ is a regularization hyperparameter.

Training Algorithm

To learn embeddings for a given ontology, we first transform the ABox axioms and normalize the TBox, as previously discussed. We then start with a random initialization of the embeddings and minimize the sum of all loss terms via mini-batch gradient descent.

3.3 Soundness

We now show that the geometric embeddings learned by Box²EL correctly encode the semantics of the given ontology, i.e., correspond to a logical model of the ontology.

Theorem 1 (Soundness). *Let $\mathcal{O} = (\mathcal{T}, \mathcal{A})$ be an \mathcal{EL}^{++} ontology. If $\gamma \leq 0$ and there exists a Box²EL configuration such that $\mathcal{L}(\mathcal{O}) = 0$, then \mathcal{O} has a model.*

Proof sketch. We construct a geometric interpretation \mathcal{I} of \mathcal{O} by interpreting every concept as the set of points in its associated box, and every role as the Cartesian product of the set of points in its head box and the set of points in its tail box. Since $\mathcal{L}(\mathcal{O}) = 0$, we have that \mathcal{I} is a model of \mathcal{O} . \square

A formal proof of Theorem 1 is given in Appendix A.

4 Experiments

We evaluate Box²EL on three tasks: subsumption prediction, link (protein-protein interaction) prediction and deductive reasoning.⁵ We have furthermore conducted a variety of ablation studies that can be found in Appendix B. Our Box²EL implementation is based on PyTorch [Paszke *et al.*, 2019]. Transforming an ontology into normal form is handled as a pre-processing step with the implementation provided by [Kulmanov *et al.*, 2019], which internally makes use of the jcel reasoner [Mendez, 2012].

4.1 Subsumption Prediction

Subsumption prediction, or *inductive reasoning*, is to predict plausible subsumptions that are not necessarily logically entailed by the given ontology. In contrast to previous work [Mondal *et al.*, 2021; Xiong *et al.*, 2022], we do not only consider subsumptions between atomic concepts, but also the more challenging task of predicting subsumptions between atomic and complex concepts.

Benchmark. We introduce a novel benchmark based on the previously considered biomedical ontologies GALEN [Rector *et al.*, 1996], Gene Ontology (GO) [Ashburner *et al.*, 2000], and Anatomy (also called Uberon) [Mungall *et al.*, 2012]. For each ontology, our benchmark consists of axioms split into training (80%), validation (10%), and testing (10%) sets for each normal form. This enables us to evaluate DL embedding models on subsumption prediction between atomic concepts (NF1), atomic concepts and conjunctions (NF2), and atomic concepts and existentially restricted concepts (NF3 and NF4).

Baselines. We compare Box²EL with the state-of-the-art \mathcal{EL}^{++} embedding methods ELEM [Kulmanov *et al.*, 2019], EmEL⁺⁺ [Mondal *et al.*, 2021], and ELBE [Peng *et al.*, 2022]. Furthermore, we are currently working on evaluating BoxEL [Xiong *et al.*, 2022] on our benchmark. We do not consider any traditional KGE methods in our experiments, since they have been shown to be considerably outperformed by DL embedding methods [Mondal *et al.*, 2021; Xiong *et al.*, 2022] and are not applicable in the setting of complex concepts.

Evaluation protocol. To evaluate the subsumption prediction performance of the embedding models, we report a variety of ranking-based metrics on the testing set. Given a test axiom in some normal form, we generate a set of candidate predictions by replacing the atomic side of the subsumption with all possible concepts in \mathcal{N}'_{CI} . We then rank all candidate predictions by a score based on the distance between the embeddings on either side of the subsumption (for details see Appendix C) and record the rank of the true axiom. We report the standard metrics Hits@ k (H@ k), where $k \in \{1, 10, 100\}$, the median rank (Med), the mean reciprocal rank (MRR), the mean rank (MR), and the area under the ROC curve (AUC). These metrics are computed for the axioms in each normal form individually, as well as combined across normal forms.

⁵All code and data is available at <https://github.com/KRR-Oxford/BoxSquaredEL/tree/v1.0.0>.

	Model	H@1	H@10	H@100	Med	MRR	MR	AUC
GALEN	ELEm	0.01	0.12	0.29	1662	0.05	5153	0.78
	EmEL ⁺⁺	0.01	0.11	0.24	2295	0.05	5486	0.76
	ELBE	0.02	0.14	0.27	1865	0.06	5303	0.77
	Box ² EL	0.04	0.18	0.36	643	0.09	4511	0.81
GO	ELEm	0.03	0.24	0.43	272	0.09	6204	0.86
	EmEL ⁺⁺	0.03	0.23	0.38	597	0.09	6710	0.85
	ELBE	0.01	0.10	0.22	1838	0.04	6986	0.85
	Box ² EL	0.04	0.23	0.60	50	0.10	3151	0.93
Anatomy	ELEm	0.10	0.40	0.64	22	0.19	6464	0.94
	EmEL ⁺⁺	0.11	0.36	0.57	36	0.19	8472	0.92
	ELBE	0.04	0.36	0.63	29	0.15	5400	0.95
	Box ² EL	0.19	0.48	0.69	13	0.29	3312	0.97

Table 1: Subsumption prediction results combined across normal forms.

Experimental protocol. The embeddings are optimized with Adam [Kingma and Ba, 2015] for a maximum of 10,000 epochs. All hyperparameters are described in detail in Appendix D. We evaluate the models on a fraction of the validation set every 100 epochs and choose the embeddings that achieve the best performance for final evaluation on the testing set. The results we report are averages across 5 runs with different random seeds, which we provide in our implementation for reproducibility. All experiments were conducted on a machine with an Intel Xeon Bronze 3204 processor with 12 cores at a clock speed of 1.90 GHz, 128 GB of RAM, and an NVIDIA Quadro RTX 8000 GPU.

Results

We report the results combined across all normal forms in Table 1. Furthermore, detailed results for each normal form on the GALEN ontology are given in Table 2. For detailed results on GO and Anatomy, see Appendix E.

We first observe that all methods perform reasonably well, even in the novel and more challenging setting of subsumption prediction with complex concepts. The baseline methods achieve similar results, although ELEm interestingly generally performs best, in contrast to previous benchmarks. Our model Box²EL consistently outperforms the baselines on all datasets, often with significant performance gains. For example, the median rank of Box²EL is more than 60% lower than the second best-performing method on GALEN, more than 80% lower on GO, and more than 40% lower on Anatomy.

The detailed results on GALEN demonstrate that the novel role representation of Box²EL not only generally improves prediction performance for axioms that include roles (NF3 and NF4), but also for NF1 and NF2 axioms. This can be explained by the fact that the different normal forms are used to optimize the *same* embeddings; i.e., if Box²EL can better represent an axiom of the form $C \sqsubseteq \exists r.D$, it will learn better embeddings for C and D , therefore also improving prediction quality for NF1 and NF2 axioms involving C and/or D . As expected, predicting axioms with only atomic concepts in NF1 is easier than predicting complex axioms.

4.2 Link Prediction

We next evaluate our model on the task of link prediction, i.e., predicting role assertions of the form $r(a, b)$. Since the ABox

	Model	H@1	H@10	H@100	Med	MRR	MR	AUC
NF1	ELEm	0.01	0.16	0.40	430	0.06	3568	0.85
	EmEL ⁺⁺	0.02	0.16	0.37	632	0.06	3765	0.84
	ELBE	0.03	0.24	0.47	138	0.10	2444	0.89
	Box ² EL	0.02	0.25	0.55	62	0.09	2039	0.91
NF2	ELEm	0.01	0.07	0.17	5106	0.03	7432	0.68
	EmEL ⁺⁺	0.01	0.07	0.15	5750	0.03	7767	0.66
	ELBE	0.03	0.06	0.11	6476	0.04	8068	0.65
	Box ² EL	0.05	0.13	0.22	3468	0.08	7246	0.69
NF3	ELEm	0.02	0.14	0.28	1479	0.05	4831	0.79
	EmEL ⁺⁺	0.02	0.11	0.22	2240	0.05	5348	0.77
	ELBE	0.03	0.14	0.25	2154	0.07	5072	0.78
	Box ² EL	0.08	0.19	0.31	1060	0.12	4530	0.80
NF4	ELEm	0.00	0.05	0.18	3855	0.02	6793	0.71
	EmEL ⁺⁺	0.00	0.04	0.12	4458	0.01	7020	0.70
	ELBE	0.00	0.03	0.07	7563	0.01	8884	0.62
	Box ² EL	0.00	0.08	0.19	3426	0.02	6806	0.71

Table 2: Detailed subsumption prediction results on GALEN.

axioms have been transformed into corresponding TBox axioms, this is equivalent to predicting subsumptions of the form $\{a\} \sqsubseteq \exists r.\{b\}$.

Datasets. We consider the protein-protein interaction (PPI) prediction task introduced in [Kulmanov *et al.*, 2019]. They provide two ontologies of PPIs in human and yeast organisms, constructed by combining the STRING database of PPIs [Szklarczyk *et al.*, 2021] with the Gene Ontology [Ashburner *et al.*, 2000]. The proteins and their interactions recorded in STRING form the ABox, while GO acts as the TBox, and is enriched with additional axioms modeling the association of proteins with functions. The task is to predict subsumptions of the form $\{P_1\} \sqsubseteq \exists \text{interacts}.\{P_2\}$, where P_1 and P_2 represent two proteins.

Baselines. We report the relevant best results from the literature for the baseline models.

Evaluation and experimental protocol. In order to evaluate our method, we use the 80%/10%/10% training, validation, and testing split of the PPI data provided by [Kulmanov *et al.*, 2019]. We compute the same ranking-based metrics as in subsumption prediction, both in the standard and filtered fashion, in which any true candidate predictions are first removed from the set of all candidate predictions before computing the ranks. The experimental protocol is also the same as in subsumption prediction.

Results. Table 3 lists the results of Box²EL and the baseline methods on the yeast and human PPI prediction datasets. Box²EL outperforms the current state of the art on all metrics except for raw Hits@10, usually with significant performance gains, demonstrating the effectiveness of Box²EL when applied to this real-life problem. The comparatively stronger results than ELBE and BoxEL, which share the same concept representation as our model, once again highlight the positive impact of our novel box-based role representation.

4.3 Deductive Reasoning

Our evaluation so far has been concerned with the setting of predicting *plausible* axioms that are not necessarily entailed

	Model	H@10	H@10 (F)	H@100	H@100 (F)	MR	MR (F)	AUC	AUC (F)
Yeast	ELEm	0.10	0.23	0.50	0.75	247	187	0.96	0.97
	EmEL ⁺⁺	0.08	0.17	0.48	0.65	336	291	0.94	0.95
	BoxEL	0.09	0.20	0.52	0.73	423	379	0.93	0.94
	ELBE	0.11	0.26	0.57	0.77	201	154	0.96	0.97
	Box ² EL	0.10	0.30	0.62	0.84	180	130	0.97	0.98
Human	ELEm	0.09	0.22	0.43	0.70	658	572	0.96	0.96
	EmEL ⁺⁺	0.04	0.13	0.38	0.56	772	700	0.95	0.95
	BoxEL	0.07	0.10	0.42	0.63	1574	1530	0.93	0.93
	ELBE	0.09	0.22	0.49	0.72	434	362	0.97	0.98
	Box ² EL	0.08	0.24	0.52	0.79	314	241	0.98	0.98

Table 3: PPI prediction results on the yeast and human datasets. Columns annotated with (F) contain filtered metrics, other columns contain raw metrics. The results for BoxEL are from [Xiong *et al.*, 2022]; all other baseline results are from [Peng *et al.*, 2022].

	Model	H@1	H@10	H@100	Med	MRR	MR	AUC
GALEN	ELEm	0.00	0.04	0.20	1807	0.01	4405	0.81
	EmEL ⁺⁺	0.00	0.04	0.18	2049	0.01	4634	0.81
	ELBE	0.00	0.06	0.16	1961	0.02	4115	0.82
	Box ² EL	0.01	0.08	0.24	1030	0.03	2825	0.88
GO	ELEm	0.00	0.04	0.22	1629	0.02	7377	0.84
	EmEL ⁺⁺	0.00	0.04	0.19	1972	0.02	7022	0.85
	ELBE	0.00	0.06	0.21	935	0.02	3846	0.92
	Box ² EL	0.00	0.08	0.50	100	0.04	1569	0.97
Anatomy	ELEm	0.00	0.07	0.28	901	0.02	7958	0.93
	EmEL ⁺⁺	0.00	0.07	0.26	1576	0.02	10976	0.90
	ELBE	0.00	0.08	0.32	336	0.03	2312	0.98
	Box ² EL	0.00	0.09	0.47	120	0.04	1178	0.99

Table 4: Deductive reasoning results on GALEN, GO, and Anatomy.

by the ontology, i.e., inductive reasoning. We now examine how well our model is able to approximate *deductive reasoning*, i.e., inferring axioms that are logical consequences of the axioms in the ontology.

Experimental Setup

We again consider the GALEN, GO, and Anatomy ontologies. Instead of splitting the axioms into separate training, validation, and testing sets, we now train the models on the entire ontology using all of its declared axioms. For evaluation, we use the standard ELK reasoner [Kazakov *et al.*, 2014] to logically infer the complete set of hidden axioms (logical consequences) for every ontology. We report the results of Box²EL and the same baseline methods considered in subsumption prediction. The evaluation and experimental protocol is also the same as in subsumption prediction. Note that the logically inferred axioms we use to test the models on deductive reasoning only include subsumptions between atomic concepts (i.e., all test subsumptions are in NF1). We split off 10% of these inferred NF1 axioms for the validation set and keep the remainder as the testing set.

Deductive reasoning with \mathcal{EL}^{++} embeddings has been previously considered in [Mondal *et al.*, 2021]. However, we find that there is significant leakage (overlap) between their testing and training sets. We therefore do not adopt their reported results, but instead reproduce the results of the baseline models.

Results. Table 4 lists the results of the deductive reasoning experiment. The baseline methods perform similarly well, with ELBE achieving slightly stronger results than the others on GO and Anatomy. Box²EL outperforms all the baselines on all the metrics across the three ontologies, with significant performance gains especially for Hits@100, median rank, and mean rank. This indicates that Box²EL is able to preserve more of the logical structure than the baselines.

Deductive vs inductive reasoning. By comparing the results in Tables 1 and 4, we observe that the embedding models generally perform better in subsumption prediction than in deductive reasoning. This can be explained by the fact that axiom prediction relies on exploiting statistical information in the data, which is precisely what embedding models are designed for, whereas deductive reasoning actually requires some amount of logical reasoning in the embedding space. We strengthen this hypothesis by looking at a concrete example in Appendix F.

5 Conclusion and Future Work

We developed Box²EL, a novel embedding method for the DL \mathcal{EL}^{++} that adopts a box-based representation for both concepts and roles. This representation is able to model complex logical constructs from \mathcal{EL}^{++} and overcomes the limitations of previous approaches in representing one-to-many, many-to-one, and many-to-many relations. We formally proved that our method is sound, i.e., correctly represents the semantics of \mathcal{EL}^{++} , and performed an extensive empirical evaluation, achieving state-of-the-art results in subsumption prediction, protein-protein interaction (link) prediction, and deductive reasoning. Furthermore, we introduced a new benchmark to evaluate the prediction performance of DL embedding methods for subsumptions involving complex concepts.

Future work could extend Box²EL to support the full range of \mathcal{EL}^{++} axioms, or even cover more expressive DLs such as *ALC* or *SRQIQ*. It could also prove fruitful to apply our model to other life science applications such as gene-disease association prediction. Generally, we believe it is important to further study embedding approaches that incorporate logical structure, both to enable efficient logical reasoning and to complement purely data-driven machine learning techniques.

Ethical Statement

All data used in this work are publicly available and there are no privacy concerns. The proposed technology neither raises any ethical issues.

Acknowledgements

This work has been supported by eBay, Samsung Research UK, and the EPSRC projects ConCur (EP/V050869/1) and UK FIRES (EP/S019111/1). Mathias Jackermeier is funded by the EPSRC Centre for Doctoral Training in Autonomous Intelligent Machines and Systems (EP/S024050/1).

References

- [Abboud *et al.*, 2020] Ralph Abboud, İsmail İlkan Ceylan, Thomas Lukasiewicz, and Tommaso Salvatori. BoxE: A box embedding model for knowledge base completion. In *Advances in Neural Information Processing Systems*, volume 33, pages 9649–9661, 2020.
- [Ashburner *et al.*, 2000] Michael Ashburner, Catherine A Ball, Judith A Blake, David Botstein, Heather Butler, J Michael Cherry, Allan P Davis, Kara Dolinski, Selina S Dwight, Janan T Eppig, et al. Gene ontology: tool for the unification of biology. *Nature genetics*, 25(1):25–29, 2000.
- [Baader *et al.*, 2005a] Franz Baader, Sebastian Brandt, and Carsten Lutz. Pushing the EL envelope. In *Proceedings of the Nineteenth International Joint Conference on Artificial Intelligence*, volume 5, pages 364–369, 2005.
- [Baader *et al.*, 2005b] Franz Baader, Ian Horrocks, and Ulrike Sattler. Description logics as ontology languages for the semantic web. In *Mechanizing mathematical reasoning*, pages 228–248. Springer, 2005.
- [Bordes *et al.*, 2013] Antoine Bordes, Nicolas Usunier, Alberto Garcia-Duran, Jason Weston, and Oksana Yakhnenko. Translating embeddings for modeling multi-relational data. In *Advances in Neural Information Processing Systems*, volume 26, 2013.
- [Chen *et al.*, 2021] Jiaoyan Chen, Pan Hu, Ernesto Jimenez-Ruiz, Ole Magnus Holter, Denvar Antonyrajah, and Ian Horrocks. OWL2Vec*: Embedding of OWL ontologies. *Machine Learning*, 110(7):1813–1845, 2021.
- [Dettmers *et al.*, 2018] Tim Dettmers, Pasquale Minervini, Pontus Stenetorp, and Sebastian Riedel. Convolutional 2D knowledge graph embeddings. In *Proceedings of the AAAI conference on artificial intelligence*, volume 32, 2018.
- [Garg *et al.*, 2019] Dinesh Garg, Shajith Ikbal, Santosh K Srivastava, Harit Vishwakarma, Hima Karanam, and L Venkata Subramaniam. Quantum embedding of knowledge for reasoning. *Advances in Neural Information Processing Systems*, 32, 2019.
- [Gutiérrez-Basulto and Schockaert, 2018] Victor Gutiérrez-Basulto and Steven Schockaert. From knowledge graph embedding to ontology embedding? An analysis of the compatibility between vector space representations and rules. In *Sixteenth International Conference on Principles of Knowledge Representation and Reasoning*, 2018.
- [Hogan *et al.*, 2021] Aidan Hogan, Eva Blomqvist, Michael Cochez, Claudia d’Amato, Gerard de Melo, Claudio Gutierrez, Sabrina Kirrane, José Emilio Labra Gayo, Roberto Navigli, Sebastian Neumaier, et al. Knowledge graphs. *ACM Computing Surveys (CSUR)*, 54(4):1–37, 2021.
- [Kazakov *et al.*, 2014] Yevgeny Kazakov, Markus Krötzsch, and František Simančík. The Incredible ELK. *Journal of Automated Reasoning*, 53(1):1–61, 2014.
- [Kingma and Ba, 2015] Diederik P. Kingma and Jimmy Ba. Adam: A method for stochastic optimization. In *3rd International Conference on Learning Representations*, 2015.
- [Kulmanov *et al.*, 2019] Maxat Kulmanov, Wang Liu-Wei, Yuan Yan, and Robert Hoehndorf. EL embeddings: Geometric construction of models for the description logic EL++. In *Proceedings of the Twenty-Eighth International Joint Conference on Artificial Intelligence*, pages 6103–6109, 2019.
- [Lehmann *et al.*, 2015] Jens Lehmann, Robert Isele, Max Jakob, Anja Jentzsch, Dimitris Kontokostas, Pablo N. Mendes, Sebastian Hellmann, Mohamed Morsey, Patrick van Kleef, Sören Auer, and Christian Bizer. DBpedia - A large-scale, multilingual knowledge base extracted from wikipedia. *Semantic Web*, 6(2):167–195, 2015.
- [Lin *et al.*, 2015] Yankai Lin, Zhiyuan Liu, Maosong Sun, Yang Liu, and Xuan Zhu. Learning entity and relation embeddings for knowledge graph completion. In *Twenty-ninth AAAI conference on artificial intelligence*, 2015.
- [Mendez, 2012] Julian Mendez. Jcel: A modular rule-based reasoner. In *Proceedings of the 1st International Workshop on OWL Reasoner Evaluation*, volume 858 of *CEUR Workshop Proceedings*, 2012.
- [Messner *et al.*, 2022] Johannes Messner, Ralph Abboud, and İsmail İlkan Ceylan. Temporal knowledge graph completion using box embeddings. In *Proceedings of the AAAI Conference on Artificial Intelligence*, volume 36, pages 7779–7787, 2022.
- [Mikolov *et al.*, 2013] Tomas Mikolov, Kai Chen, Greg Corrado, and Jeffrey Dean. Efficient estimation of word representations in vector space. *arXiv preprint*, 2013.
- [Mondal *et al.*, 2021] Sutapa Mondal, Sumit Bhatia, and Raghava Mutharaju. EmEL++: Embeddings for \mathcal{EL}^{++} Description Logic. In *Proceedings of the AAAI 2021 Spring Symposium on Combining Machine Learning and Knowledge Engineering*, volume 2846 of *CEUR Workshop Proceedings*, 2021.
- [Mungall *et al.*, 2012] Christopher J. Mungall, Carlo Torniai, Georgios V. Gkoutos, Suzanna E. Lewis, and Melissa A. Haendel. Uberon, an integrative multi-species anatomy ontology. *Genome Biology*, 13(1):R5, 2012.
- [Nickel and Kiela, 2017] Maximillian Nickel and Douwe Kiela. Poincaré embeddings for learning hierarchical rep-

- resentations. In *Advances in Neural Information Processing Systems*, volume 30, pages 6338–6347, 2017.
- [Paszke *et al.*, 2019] Adam Paszke, Sam Gross, Francisco Massa, Adam Lerer, James Bradbury, Gregory Chanan, Trevor Killeen, Zeming Lin, Natalia Gimelshein, Luca Antiga, Alban Desmaison, Andreas Kopf, Edward Yang, Zachary DeVito, Martin Raison, Alykhan Tejani, Sasank Chilamkurthy, Benoit Steiner, Lu Fang, Junjie Bai, and Soumith Chintala. PyTorch: An imperative style, high-performance deep learning library. In *Advances in Neural Information Processing Systems*, volume 32, pages 8024–8035, 2019.
- [Peng *et al.*, 2022] Xi Peng, Zhenwei Tang, Maxat Kulmanov, Kexin Niu, and Robert Hoehndorf. Description logic \mathcal{EL}^{++} embeddings with intersectional closure. *arXiv preprint*, 2022.
- [Rector *et al.*, 1996] Alan L Rector, Jeremy E Rogers, and Pam Pole. The GALEN high level ontology. In *Medical Informatics Europe '96*, pages 174–178. IOS Press, 1996.
- [Ristoski and Paulheim, 2016] Petar Ristoski and Heiko Paulheim. RDF2Vec: RDF graph embeddings for data mining. In *International Semantic Web Conference*, pages 498–514. Springer, 2016.
- [Smaili *et al.*, 2019] Fatima Zohra Smaili, Xin Gao, and Robert Hoehndorf. OPA2Vec: Combining formal and informal content of biomedical ontologies to improve similarity-based prediction. *Bioinformatics*, 35(12):2133–2140, 2019.
- [Staab and Studer, 2010] Steffen Staab and Rudi Studer. *Handbook on ontologies*. Springer Science & Business Media, 2010.
- [Szkarczyk *et al.*, 2021] Damian Szkarczyk, Annika L Gable, Katerina C Nastou, David Lyon, Rebecca Kirsch, Sampo Pyysalo, Nadezhda T Doncheva, Marc Legeay, Tao Fang, Peer Bork, Lars J Jensen, and Christian von Mering. The STRING database in 2021: Customizable protein–protein networks, and functional characterization of user-uploaded gene/measurement sets. *Nucleic Acids Research*, 49(D1):D605–D612, 2021.
- [Vilnis *et al.*, 2018] Luke Vilnis, Xiang Li, Shikhar Murty, and Andrew McCallum. Probabilistic embedding of knowledge graphs with box lattice measures. In *Proceedings of the 56th Annual Meeting of the Association for Computational Linguistics (Volume 1: Long Papers)*, pages 263–272, 2018.
- [Vrandečić and Krötzsch, 2014] Denny Vrandečić and Markus Krötzsch. Wikidata: a free collaborative knowledgebase. *Communications of the ACM*, 57(10):78–85, 2014.
- [Wang *et al.*, 2014] Zhen Wang, Jianwen Zhang, Jianlin Feng, and Zheng Chen. Knowledge graph embedding by translating on hyperplanes. In *Proceedings of the AAAI conference on artificial intelligence*, volume 28, 2014.
- [Wang *et al.*, 2017] Quan Wang, Zhendong Mao, Bin Wang, and Li Guo. Knowledge graph embedding: A survey of approaches and applications. *IEEE Transactions on Knowledge and Data Engineering*, 29(12):2724–2743, 2017.
- [Xiong *et al.*, 2022] Bo Xiong, Nico Potyka, Trung-Kien Tran, Mojtaba Nayyeri, and Steffen Staab. Faithful embeddings for \mathcal{EL}^{++} knowledge bases. In *Proceedings of the 21st International Semantic Web Conference*, volume 13489 of *Lecture Notes in Computer Science*, pages 22–38. Springer, 2022.
- [Yang *et al.*, 2015] Bishan Yang, Scott Wen-tau Yih, Xiaodong He, Jianfeng Gao, and Li Deng. Embedding entities and relations for learning and inference in knowledge bases. In *Proceedings of the International Conference on Learning Representations*, 2015.

A Proof of Theorem 1 (Soundness)

In order to prove Theorem 1, we first need to formally show the correctness of our loss functions.

Lemma 1. Recall that the inclusion loss $\mathcal{L}_{\subseteq}(A, B)$ of two boxes A and B is defined as

$$\|\max\{\mathbf{0}, d(A, B) + 2o(A) - \gamma\}\|.$$

If $\mathcal{L}_{\subseteq}(A, B) = 0$ and $\gamma \leq 0$, then $A \subseteq B$.

Proof. We prove the lemma by showing that $\mathbf{l}_B \leq \mathbf{l}_A$ and $\mathbf{u}_A \leq \mathbf{u}_B$, where \mathbf{l} and \mathbf{u} denote the lower and upper corner of the relevant box, respectively. Assume $\mathcal{L}_{\subseteq}(A, B) = 0$. We have that

$$\begin{aligned} d(A, B) + 2o(A) - \gamma &\leq 0 \\ |c(A) - c(B)| + o(A) - o(B) - \gamma &\leq 0 \end{aligned}$$

and thus

$$|c(A) - c(B)| + o(A) - o(B) \leq \gamma \leq 0.$$

Now fix an arbitrary dimension k such that $1 \leq k \leq n$. We distinguish two cases:

Case 1: $c(A)_k \geq c(B)_k$. We eliminate the absolute value function and use $\mathbf{u}_\beta = c(\beta) + o(\beta)$ for an arbitrary box β to obtain

$$\begin{aligned} \mathbf{u}_{A,k} - \mathbf{u}_{B,k} &\leq 0 \\ \mathbf{u}_{A,k} &\leq \mathbf{u}_{B,k}. \end{aligned}$$

Since $c(A)_k \geq c(B)_k$, we furthermore have by the definition of $c(\cdot)$ that

$$\begin{aligned} \frac{\mathbf{l}_{A,k} + \mathbf{u}_{A,k}}{2} &\geq \frac{\mathbf{l}_{B,k} + \mathbf{u}_{B,k}}{2} \\ \mathbf{l}_{A,k} &\geq \mathbf{l}_{B,k} + \underbrace{\mathbf{u}_{B,k} - \mathbf{u}_{A,k}}_{\geq 0} \\ \mathbf{l}_{A,k} &\geq \mathbf{l}_{B,k}. \end{aligned}$$

Case 2: $c(A)_k \leq c(B)_k$. Similarly to the first case, we eliminate the absolute value function and use $\mathbf{l}_\beta = c(\beta) - o(\beta)$ to obtain

$$\begin{aligned} -\mathbf{l}_{A,k} + \mathbf{l}_{B,k} &\leq 0 \\ \mathbf{l}_{B,k} &\leq \mathbf{l}_{A,k}. \end{aligned}$$

Because $c(A)_k \leq c(B)_k$, we furthermore have

$$\begin{aligned} \frac{\mathbf{l}_{A,k} + \mathbf{u}_{A,k}}{2} &\leq \frac{\mathbf{l}_{B,k} + \mathbf{u}_{B,k}}{2} \\ \underbrace{\mathbf{l}_{A,k} - \mathbf{l}_{B,k}}_{\geq 0} + \mathbf{u}_{A,k} &\leq \mathbf{u}_{B,k} \\ \mathbf{u}_{A,k} &\leq \mathbf{u}_{B,k}. \end{aligned}$$

Now, consider an arbitrary point $\mathbf{a} \in A$, i.e., $\mathbf{l}_A \leq \mathbf{a} \leq \mathbf{u}_A$. But then

$$\mathbf{l}_B \leq \mathbf{l}_A \leq \mathbf{a} \leq \mathbf{u}_A \leq \mathbf{u}_B$$

and thus $\mathbf{a} \in B$. \square

Lemma 2. Let A and B be boxes in \mathbb{R}^n and $\gamma \leq 0$. If

$$\|\max\{\mathbf{0}, -(d(A, B) + \gamma)\}\| = 0,$$

then $A \cap B = \emptyset$.

Proof. The proof is similar to Lemma 1. We have that

$$\begin{aligned} -(d(A, B) + \gamma) &\leq 0 \\ -(|c(A) - c(B)| - o(A) - o(B) + \gamma) &\leq 0 \end{aligned}$$

and therefore

$$|c(A) - c(B)| - o(A) - o(B) \geq -\gamma \geq 0.$$

We again fix a dimension k such that $1 \leq k \leq n$ and distinguish two cases:

Case 1: $c(A)_k \geq c(B)_k$. Eliminating the absolute value function yields

$$\begin{aligned} \mathbf{l}_{A,k} - \mathbf{u}_{B,k} &\geq 0 \\ \mathbf{l}_{A,k} &\geq \mathbf{u}_{B,k}. \end{aligned} \quad (1)$$

Case 2: $c(A)_k \leq c(B)_k$. Analogously to Case 1, we have

$$\begin{aligned} \mathbf{l}_{B,k} - \mathbf{u}_{A,k} &\geq 0 \\ \mathbf{l}_{B,k} &\geq \mathbf{u}_{A,k}. \end{aligned} \quad (2)$$

Now consider an arbitrary point $\mathbf{a} \in A$. From the case analysis above, we know that either $\mathbf{a}_k \geq \mathbf{u}_{B,k}$ or $\mathbf{a}_k \leq \mathbf{l}_{B,k}$. However, in both cases \mathbf{a} cannot be in B . \square

We are now ready to prove Theorem 1, restated below.

Theorem 1 (Soundness). Let $\mathcal{O} = (\mathcal{T}, \mathcal{A})$ be an \mathcal{EL}^{++} ontology. If $\gamma \leq 0$ and there exists a Box^2EL configuration such that $\mathcal{L}(\mathcal{O}) = 0$, then \mathcal{O} has a model.

Proof. We first perform the standard steps of transforming the ABox and normalising the axioms in \mathcal{O} . Let \mathcal{O}' denote the resulting ontology. Consider the geometric interpretation $\mathcal{I} = (\Delta^{\mathcal{I}}, \cdot^{\mathcal{I}})$, induced by the Box^2EL configuration:

1. $\Delta^{\mathcal{I}} = \mathbb{R}^n$,
2. for every concept $C \in \mathcal{N}'_{CI}$, let $C^{\mathcal{I}} = \text{Box}(C)$,
3. for every role $r \in \mathcal{N}'_R$, let $r^{\mathcal{I}} = \text{Head}(r) \times \text{Tail}(r)$.

We show that \mathcal{I} is a model of \mathcal{O}' . First, note that $\mathcal{L}(\mathcal{O}) = 0$ implies that the regularization loss is 0, and thus $\text{Bump}(C) = \mathbf{0}$ for any $C \in \mathcal{N}'_{CI}$. We now show that \mathcal{I} satisfies every axiom $\alpha \in \mathcal{O}'$, distinguishing between the different normal forms. Implicitly, we make frequent use of Lemma 1, which we do not state explicitly for the sake of brevity.

Case 1: $\alpha = C \sqsubseteq D$. Since $\mathcal{L}_1(C, D) = 0$ and therefore $\mathcal{L}_{\subseteq}(\text{Box}(C), \text{Box}(D)) = 0$, we have that $\text{Box}(C) \subseteq \text{Box}(D)$. But then it immediately follows from the definition of \mathcal{I} that $C^{\mathcal{I}} \subseteq D^{\mathcal{I}}$.

Case 2: $\alpha = C \sqcap D \sqsubseteq E$. We have that $\mathcal{L}_2(C, D, E) = 0$ and therefore it follows that $\text{Box}(C) \cap \text{Box}(D) \subseteq \text{Box}(E)$. Hence, we have $(C \sqcap D)^{\mathcal{I}} = C^{\mathcal{I}} \cap D^{\mathcal{I}} = \text{Box}(C) \cap \text{Box}(D) \subseteq \text{Box}(E) = E^{\mathcal{I}}$.

Case 3: $\alpha = C \sqsubseteq \exists r.D$. Let $x \in C^{\mathcal{I}} = \text{Box}(C)$. Since $\mathcal{L}_3(C, r, D) = 0$ and all bump vectors are $\mathbf{0}$, we have $\text{Box}(C) \subseteq \text{Head}(r)$ and therefore $x \in \text{Head}(r)$. Similarly, for any $y \in D^{\mathcal{I}}$ we have $y \in \text{Tail}(r)$. But then $(x, y) \in r^{\mathcal{I}}$ and therefore $x \in (\exists r.D)^{\mathcal{I}}$.

	Model	H@1	H@10	H@100	Med	MRR	MR	AUC
NF1	Box ² EL-TE	0.02	0.22	0.45	159	0.08	2417	0.90
	Box ² EL	0.02	0.25	0.55	62	0.09	2039	0.91
NF2	Box ² EL-TE	0.02	0.05	0.13	5314	0.03	7510	0.68
	Box ² EL	0.05	0.13	0.22	3468	0.08	7246	0.69
NF3	Box ² EL-TE	0.01	0.08	0.19	2544	0.03	5623	0.76
	Box ² EL	0.08	0.19	0.31	1060	0.12	4530	0.80
NF4	Box ² EL-TE	0.00	0.02	0.09	4260	0.01	7092	0.69
	Box ² EL	0.00	0.08	0.19	3426	0.02	6806	0.71
All	Box ² EL-TE	0.01	0.11	0.25	1557	0.05	5099	0.78
	Box ² EL	0.04	0.18	0.36	643	0.09	4511	0.81

Table 5: Impact of the role representation on the performance of Box²EL. We compare our model with a version in which roles are represented via TransE (Box²EL-TE).

Case 4: $\alpha = \exists r.C \sqsubseteq D$. Let $x \in (\exists r.C)^{\mathcal{I}}$. Hence, there exist a $y \in C^{\mathcal{I}}$ such that $(x, y) \in r^{\mathcal{I}}$. By the definition of $r^{\mathcal{I}}$, we must therefore have $x \in \text{Head}(r)$. Since $\mathcal{L}_4(r, C, D) = 0$, furthermore $\text{Head}(r) \subseteq \text{Box}(D)$ and therefore $x \in D^{\mathcal{I}}$.

Case 5: $\alpha = C \sqcap D \sqsubseteq \perp$. We have $\mathcal{L}_5(C, D) = 0$, so by Lemma 2 we have that $(C \sqcap D)^{\mathcal{I}} = \text{Box}(C) \cap \text{Box}(D) = \emptyset \subseteq \perp^{\mathcal{I}}$.

Case 6: $\alpha = \exists r.C \sqsubseteq \perp$. The loss $\mathcal{L}_6(r, C) = 0$ implies that $\text{Head}(r) = \emptyset$. Therefore $r^{\mathcal{I}} = \emptyset$, which means $(\exists r.C)^{\mathcal{I}} = \emptyset$ and hence $(\exists r.C)^{\mathcal{I}} \subseteq \perp^{\mathcal{I}}$.

Case 7: $\alpha = C \sqsubseteq \perp$. We have that $\mathcal{L}_7(C) = 0$, from which we immediately obtain $\text{Box}(C) = \emptyset$. Thus, $C^{\mathcal{I}} \subseteq \perp^{\mathcal{I}}$.

We have shown that \mathcal{I} satisfies every axiom in \mathcal{O}' , and is therefore a model of \mathcal{O}' . But since \mathcal{O}' is a conservative extension of \mathcal{O} [Baader *et al.*, 2005a], it follows that \mathcal{I} is also a model of \mathcal{O} . \square

B Ablation Studies

We conduct a variety of ablation studies to investigate the performance of different parts of our model. All studies are conducted on the GALEN ontology for the subsumption prediction task.

B.1 Impact of Role Representation

One novel contribution of Box²EL is its role representation based on BoxE. We have illustrated the conceptual advantages of this role representation and argued that it is a key ingredient for the performance of our model. To strengthen these claims, we conduct an ablation study in which we replace our role representation with TransE, and keep the rest of our model exactly the same. The results are given in Table 5.

We observe that the model based on BoxE outperforms the TransE-based model on all metrics, in most cases by a large margin. Furthermore, we again see that the box-based role representation improves results not only for axioms involving roles (i.e. axioms in NF3 or NF4), but consistently across the different normal forms. As noted earlier, this is due to the fact that the axioms in different normal forms are used to optimize the same concept embeddings. Overall, it is clear that the

Model	H@1	H@10	H@100	Med	MRR	MR	AUC
Box ² EL-NB	0.00	0.03	0.12	7336	0.01	8673	0.63
Box ² EL-NR	0.04	0.16	0.33	877	0.08	4789	0.79
Box ² EL	0.04	0.18	0.36	643	0.09	4511	0.81

Table 6: Impact of bump vectors and regularisation on the performance of Box²EL. We compare our model with a version without bump vectors (Box²EL-NB) and a version without regularization (Box²EL-NR).

Model	H@1	H@10	H@100	Med	MRR	MR	AUC
Box ² EL-0	0.00	0.02	0.10	7805	0.01	8925	0.61
Box ² EL-1	0.04	0.19	0.35	694	0.09	4501	0.81
Box ² EL-2	0.04	0.18	0.36	643	0.09	4511	0.81
Box ² EL-3	0.04	0.18	0.36	635	0.08	4513	0.81

Table 7: Impact of the number of negative samples on the performance of Box²EL. The model Box²EL- k denotes Box²EL trained with k negative samples per axiom in NF3.

novel role representation is indeed crucially important for the performance of our model.

B.2 Bump Vectors and Regularization

The second ablation study we conduct concerns the details of our role representation. As in BoxE, a central feature of our representation is the use of bump vectors, which enable the embeddings of concepts to dynamically adapt to different roles. In Table 6, we investigate the performance of a model without bump vectors, and a model that uses unregularized bump vectors. The results are combined across all normal forms.

We observe that the model without bump vectors significantly underperforms, highlighting that they are an important component of our model. Furthermore, we see that regularization consistently improves our results across all metrics, suggesting that it successfully reduces overfitting.

B.3 Number of Negative Samples

Finally, we investigate the impact of the number of negative samples on the performance of our model. Table 7 lists the results achieved by various Box²EL models trained with $\omega \in \{0, 1, 2, 3\}$ negative samples per axiom in NF3.

Comparing the results of the model that was trained without any negative samples to the others, we see that it performs significantly worse. This demonstrates that negative sampling is essential to learn strong embeddings. Increasing the number ω of negative samples improves the results on some metrics, but not on all. We find that a number of 2–3 negative samples generally performs best.

C Scoring Functions

Scoring functions are used to compute the likelihood of candidate axioms based on the learned embeddings of their concepts. We define a scoring function $s(\cdot)$ for candidate axioms in all four normal forms NF1–4.

	Model	n	γ	lr	δ	ω	λ
GALEN	ELEm	200	0.05	5×10^{-4}	–	–	–
	EmEL ⁺⁺	200	0.05	5×10^{-4}	–	–	–
	ELBE	200	0.05	5×10^{-3}	–	–	–
	Box ² EL	200	0.05	1×10^{-3}	2	2	0.05
GO	ELEm	200	0.1	5×10^{-4}	–	–	–
	EmEL ⁺⁺	200	0.1	5×10^{-4}	–	–	–
	ELBE	200	0.1	5×10^{-3}	–	–	–
	Box ² EL	200	0.05	5×10^{-3}	3	3	0.05
Anatomy	ELEm	200	0.05	5×10^{-4}	–	–	–
	EmEL ⁺⁺	200	0.05	5×10^{-4}	–	–	–
	ELBE	200	0.05	5×10^{-3}	–	–	–
	Box ² EL	200	0.05	1×10^{-3}	2	2	0.05

Table 8: Hyperparameters for the subsumption prediction task.

First and second normal form. For an NF1 axiom $C \sqsubseteq D$, the score is based simply on the distance between the embeddings of C and D , i.e., for Box²EL we have

$$s(C \sqsubseteq D) = -\|c(\text{Box}(C)) - c(\text{Box}(D))\|.$$

The same formulation can be used for the baseline methods. Similarly, for NF2 axioms $C \sqcap D \sqsubseteq E$, the score is defined as the negative distance of the embedding of E to the intersection of C and D in the embedding space.

Third normal form. For axioms in the third and fourth normal form the scoring function differs between Box²EL and the baseline methods, because of the different role representation. For Box²EL, the score for a subsumption $C \sqsubseteq \exists r.D$ is naturally defined as

$$s(C \sqsubseteq \exists r.D) = -\|c(\text{Box}(C)) + \text{Bump}(D) - c(\text{Head}(r))\| - \|c(\text{Box}(D)) + \text{Bump}(C) - c(\text{Tail}(r))\|.$$

In the baseline methods, the score is computed similarly to TransE:

$$s(C \sqsubseteq \exists r.D) = -\|c(\text{Box}(C)) + v(r) - c(\text{Box}(D))\|,$$

where $v(r)$ is the embedding of role r .

Fourth normal form. Finally, for an NF4 axiom $\exists r.C \sqsubseteq D$, the score assigned by Box²EL is given by

$$s(\exists r.C \sqsubseteq D) = -\|c(\text{Head}(r)) - \text{Bump}(C) - c(\text{Box}(D))\|,$$

and for the baseline methods we have

$$s(\exists r.C \sqsubseteq D) = -\|c(\text{Box}(C)) - v(r) - c(\text{Box}(D))\|.$$

D Hyperparameters

For all experiments, embeddings are learned with the Adam optimizer [Kingma and Ba, 2015] for a maximum of 10,000 epochs. All hyperparameters are selected based on validation set performance. The values considered are: dimensionality $n \in \{50, 100, 200\}$, margin $\gamma \in \{0, 0.05, 0.1\}$, learning rate $\text{lr} \in \{1 \times 10^{-2}, 5 \times 10^{-3}, 1 \times 10^{-3}, 5 \times 10^{-4}\}$, negative sampling distance $\delta \in \{1, 2, 3\}$, number of negative samples $\omega \in \{1, 2, 3\}$, and regularization $\lambda \in \{0, 0.05, 0.1\}$.

	Model	n	γ	lr	δ	ω	λ
GALEN	ELEm	200	0	5×10^{-4}	–	–	–
	EmEL ⁺⁺	200	0	5×10^{-4}	–	–	–
	ELBE	200	0.1	5×10^{-3}	–	–	–
	Box ² EL	200	0.05	5×10^{-3}	1	2	0
GO	ELEm	200	0.1	1×10^{-3}	–	–	–
	EmEL ⁺⁺	200	0.1	1×10^{-3}	–	–	–
	ELBE	200	0.05	5×10^{-3}	–	–	–
	Box ² EL	200	0.05	5×10^{-3}	3	3	0.05
Anatomy	ELEm	200	0.05	5×10^{-4}	–	–	–
	EmEL ⁺⁺	200	0.05	5×10^{-4}	–	–	–
	ELBE	200	0.05	5×10^{-3}	–	–	–
	Box ² EL	200	0.05	1×10^{-3}	2	2	0.05

Table 9: Hyperparameters for the deductive reasoning task.

	n	γ	lr	δ	ω	λ
Yeast	200	0.05	1×10^{-2}	3	3	0.05
Human	200	0.05	5×10^{-3}	3	3	0.05

Table 10: Hyperparameters for the PPI prediction task.

We report the hyperparameters used in the experiments in Tables 8 to 10. Note that for ELBE on GALEN in subsumption prediction and for Box²EL on GALEN in deductive reasoning, we furthermore decay the learning rate by a factor of 0.1 after 2000 training epochs. For PPI prediction, we only report the hyperparameters for Box²EL, since the baseline results are taken from the literature.

E Further Experimental Results

We report detailed results for each normal form for subsumption prediction on GO and Anatomy in Tables 11 and 12, respectively.

F Comparison of Deductive and Inductive Reasoning

We investigate the comparatively lower performance of the embedding models on deductive reasoning compared to the (inductive) subsumption prediction task with a concrete example. In the GALEN ontology, we find the following subsumption axiom to predict in the testing set:

$$\text{SodiumLactate} \sqsubseteq \text{NAMEDComplexChemical}.$$

This axiom cannot be logically inferred from the training data. However, the following similar subsumptions are part of the training data:

$$\begin{aligned} \text{SodiumLactate} &\sqsubseteq \exists \text{isMadeOf.Sodium} \\ \text{SodiumBicarbonate} &\sqsubseteq \exists \text{isMadeOf.Sodium} \\ \text{SodiumCitrate} &\sqsubseteq \exists \text{isMadeOf.Sodium} \\ \text{SodiumBicarbonate} &\sqsubseteq \text{NAMEDComplexChemical} \\ \text{SodiumCitrate} &\sqsubseteq \text{NAMEDComplexChemical}. \end{aligned}$$

	Model	H@1	H@10	H@100	Med	MRR	MR	AUC
NF1	ELEm	0.01	0.13	0.35	590	0.05	6433	0.86
	EmEL ⁺⁺	0.01	0.12	0.30	1023	0.05	6709	0.85
	ELBE	0.01	0.10	0.24	1156	0.04	5657	0.88
	Box ² EL	0.03	0.16	0.59	61	0.08	2616	0.94
NF2	ELEm	0.12	0.49	0.63	11	0.24	4508	0.90
	EmEL ⁺⁺	0.11	0.44	0.55	23	0.21	5169	0.89
	ELBE	0.01	0.05	0.09	6456	0.02	9421	0.80
	Box ² EL	0.22	0.65	0.77	5	0.36	1546	0.97
NF3	ELEm	0.06	0.40	0.52	54	0.15	6292	0.86
	EmEL ⁺⁺	0.05	0.39	0.48	210	0.15	7788	0.83
	ELBE	0.02	0.15	0.30	959	0.07	7131	0.84
	Box ² EL	0.00	0.14	0.51	90	0.04	5074	0.89
NF4	ELEm	0.01	0.49	0.60	12	0.12	6272	0.86
	EmEL ⁺⁺	0.01	0.49	0.58	12	0.13	6442	0.86
	ELBE	0.00	0.07	0.12	9049	0.02	12868	0.72
	Box ² EL	0.00	0.45	0.66	14	0.10	4960	0.89

Table 11: Detailed subsumption prediction results on GO.

It seems quite likely that our model will be able to exploit the statistical information contained in these subsumptions to learn embeddings where SodiumLactate is close to NAMED-ComplexChemical, and thus achieve a high score for the desired true axiom.

In contrast, in the deductive reasoning setting, all testing axioms are logical inferences of the training data. One such testing axiom is

$$\text{SodiumLactate} \sqsubseteq \text{SodiumCompound}.$$

This logical inference has been reached by a reasoning algorithm such as ELK by performing the sequence of derivations listed in Figure 3. In order to perform the same reasoning in the embedding space, the embeddings learned by our model have to be highly accurate for a number of different concepts and roles such as SodiumLactate, isMadeOf, Sodium, and SodiumCompound, to name but a few examples from the last derivation. Furthermore, the scoring functions we use are based only on the distances between concepts and do not take the rich logical structure of such derivations into account.

It is thus apparent that deductive reasoning with embeddings is an inherently more challenging task than inductive reasoning (a.k.a. prediction), and it comes as no surprise that the embedding models generally perform worse on this task. However, we are confident that future research will be able to address some of the shortcomings we have identified above and better approximate deductive reasoning in the embedding space.

	Model	H@1	H@10	H@100	Med	MRR	MR	AUC
NF1	ELEm	0.07	0.30	0.57	43	0.14	9059	0.91
	EmEL ⁺⁺	0.08	0.29	0.53	60	0.14	10414	0.90
	ELBE	0.05	0.24	0.55	68	0.11	5177	0.95
	Box ² EL	0.04	0.25	0.62	39	0.11	4367	0.96
NF2	ELEm	0.03	0.18	0.42	394	0.08	11592	0.89
	EmEL ⁺⁺	0.03	0.18	0.35	1291	0.08	15759	0.85
	ELBE	0.02	0.11	0.26	1394	0.05	4885	0.96
	Box ² EL	0.13	0.34	0.55	66	0.20	2465	0.98
NF3	ELEm	0.12	0.47	0.69	13	0.23	4686	0.96
	EmEL ⁺⁺	0.13	0.42	0.60	23	0.23	7097	0.93
	ELBE	0.04	0.44	0.70	16	0.18	5408	0.95
	Box ² EL	0.30	0.62	0.75	4	0.41	2612	0.98
NF4	ELEm	0.00	0.03	0.23	813	0.01	10230	0.91
	EmEL ⁺⁺	0.00	0.02	0.17	1470	0.01	10951	0.90
	ELBE	0.00	0.02	0.06	6261	0.01	15187	0.86
	Box ² EL	0.00	0.07	0.25	615	0.02	6166	0.94

Table 12: Detailed subsumption prediction results on Anatomy.

$$\begin{array}{rcl}
 \text{SodiumLactate} \sqsubseteq \text{NAMEDComplexChemical} & \text{NAMEDComplexChemical} \sqsubseteq \text{ChemicalSubstance} & \\
 \hline
 \text{SodiumLactate} \sqsubseteq \text{ChemicalSubstance} & & (3) \\
 \\
 \text{SodiumLactate} \sqsubseteq \exists \text{isMadeOf.Sodium} & & (4) \\
 \\
 \begin{array}{rcl}
 (3) & (4) & \text{ChemicalSubstance} \sqcap \exists \text{isMadeOf.Sodium} \sqsubseteq \text{SodiumCompound} \\
 \hline
 \text{SodiumLactate} \sqsubseteq \text{SodiumCompound} & & (5)
 \end{array}
 \end{array}$$

Figure 3: Inference steps required to derive $\text{SodiumLactate} \sqsubseteq \text{SodiumCompound}$. The derivations are from top to bottom, similar to natural deduction.